Static and Dynamic Design Methods for Hybrid Bolted Joints in a Satellite Structure

Calin-Dumitru COMAN*

*Corresponding author
INCAS – National Institute for Aerospace Research "Elie Carafoli",
B-dul Iuliu Maniu 220, Bucharest 061126, Romania,
coman.calin@incas.ro

DOI: 10.13111/2066-8201.2018.10.2.17

Received: 16 February 2018/ Accepted: 24 April 2018/ Published: June 2018

Abstract: *A detailed analytical design for hybrid (metal-composite) bolted joints in static and dynamic (random vibrations) analysis is presented in this paper. Due to the fact that a space structure must be lighter and stiffened, the joints design represents an important aspect in the overall mass-stiffness optimization process of the structure. The hybrid joint studied represents the attachment between a real space thruster bracket structure made from aluminum alloy and a composite spacecraft platform subjected to quasi-static and dynamic loads. These computing techniques, originally designed for metal joints, were translated to hybrid metal-composite joints using the finite element method (FEM). As a result, using the FEM technique, the design methods proposed have validated the ability to incorporate and describe in detail the effects of important phenomena such as clamping, friction, clearance and secondary bending of the joint, which are complex three-dimensional phenomena of major importance in the design process of a hybrid joint.*

Key Words*: Bolted hybrid joints, relative sliding, pretension bolts, static, random vibrations, PATRAN-NASTRAN, laminated composites*

1. INTRODUCTION

Space engineering involves designing a structure with stiffness and strength to mass ratios as large as possible, which means considerable structural optimization. Such a performance condition of the space structures is achieved using composite materials as much as possible, as they are recognized for their exceptional strength and stiffness qualities at lower mass.

Any structure is built up from subassemblies joined together using bolts and / or rivets which represent the introduction of stress concentrators and these attachments must be treated with careful attention. Through the optimization of joints, the uncertainties in the space structure design process are reduced and experimental test cost is minimized.

Liang Ke [1] proposed a global-local FEM technique predicting strength capability for hybrid composite-to-metal bolted connections used in aerospace engineering. He studied the behavior of preloaded bolted single lap joints from composite cap in upper stage of Ariane 5ME using the same concept of margin of safety (MoS) as in the current paper. Lecomte et al. [2] presented an analytical model for prediction of stiffness and load transfer in multi-bolt composite-to-metal double lap joints. He's model is an extension of the classical spring based model for load transfer prediction, though this model has some drawbacks, one of

them is the unidirectional stiffness assumption of the plates, this being the reason for using the FEM analysis in current paper for stiffness and load transfer in a multi-bolt, double lap hybrid joint. The load distribution in multi-bolt composite joints has been investigated also by P.J. Gray and C.T. McCarthy [3] using a novel and simple FEM technique to account for tridimensional contact between the bolt shank and the hole surface, friction between the composite plates and bolt-hole clearance.

Nowadays, the worldwide application of composite materials in combination with metallic parts in modern engineering structures has led to a new structural concept called hybrid structures. In general, the hybrid metal-composite structures are divided into three main groups including steel / composite, titanium / composite and aluminum / composite, the third type being studied in this paper. In the past few years, the academic research topics in hybrid joints field included the effects of using different metal materials [4], global-local finite element techniques [1], experimental data for dynamic test [5] and temperature effect on the global failure criterion of hybrid joints [6].

The shear joints are divided into two categories depending on the occurrence of this phenomenon, namely joints in which the shear force is transmitted only by means of the frictional forces between the plates, the relative sliding being prevented, the bolt not being subjected to shear, and joints through which the shear force is transmitted through the bolt, with the occurrence of the relative sliding phenomenon between the plates.

The first category of joints is called “friction grip joints”; these joints are characterized by high torque level to induce sufficient compressive force on the plates, thus a high friction force between the plates, to prevent their relative sliding.

The second category of joints is called 'bearing joints' and the joints are characterized by small torque level, low frictional force between plates, which results in the relative sliding of the plates. In these joints, the bolt is subjected to shear load and the plates are in contact with the inner surface of the hole.

This paper proposes a complete set of analytical equations for predicting the strength of hybrid aluminum-composite joints using a thruster bracket space structure as a practical application. The methods proposed incorporate a FEM model for numerical predictions of the static and dynamic loads (bearing loads) which then are used to calculate the margins of safety for the strength evaluation. The FEM model was created in PATRAN-NASTRAN commercial software using 2D shell (for bracket structure), 1D beam (for bolts) and 0D elements (for concentrated mass as bracket thrusters).

The aim of this paper is to achieve a fully compliance of the analytical design methods for metal joints with the more restrictive and complex requirements of the hybrid metal-composite joints using 2D FEM approach.

2. PROBLEM DESCRIPTION

The satellite structure studied represents a support (bracket) for four satellite rocket thrusters, presented in Fig. 1. The structure of the bracket is made of aluminum alloy, namely AA 7075 T7351 [7] with mechanical properties presented in Table 1 and is attached to the composite satellite platform of laminated CFRP (Carbon Fiber Reinforced Polymer) having the stacking lay-up $[-45/0/+45/90]_{4s}$ with orthotropic material axis being the same as the global coordinate system axis shown in Fig.1 and material properties presented in Table 2. The attachment with the composite plate is made using standard bolts with 4 mm diameter and self-locking nuts. To prevent damage to the composite, a metal unthreaded insert is installed in the passing hole.

The structure of the bracket is subjected to quasi-static loads (QSL), presented in Table 3, that are accelerations equal to 30g (g = 9.81 m / s^2, gravitational acceleration) on each axis of the global coordinate system having the origin in the satellite center.

The second type of loads is derived from a random vibration environment, introduced using ASD (Acceleration Spectral Density) diagram; it is defined in Table 4 and illustrated in Fig. 2.

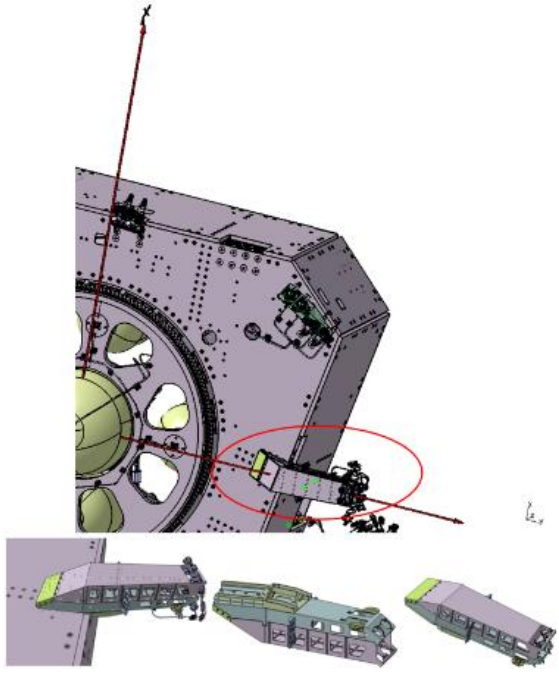

Fig. 1 Satellite structure, bracket

Table 1. Aluminum material properties, [7]

Elastic modulus E (MPa)	Poisson coefficient ν	Tensile strength σ_u (MPa)
71000	0.33	475

Table 2. CFRP orthotropic material properties

E_{11}(GPa)	E_{22}(GPa)	E_{33}(GPa)	G_{12}(GPa)	G_{13}(GPa)	G_{23}(GPa)	ν_{12}	ν_{13}	ν_{23}
150	12	12	6	6	4.3	0.3	0.3	0.4

Note: E_{ii} – elastic modulus, G_{ij} – shear modulus, ν_{ij} – coefficient, orthotropic axes are the same as global system axes.

Table 3. Quasi-static loads

Load Case	X axis	Y axis	Z axis
QSL_+X+Y+Z	30g	30g	30g
QSL_+X+Y-Z	30g	30g	-30g
QSL_+X-Y+Z	30g	-30g	30g
QSL_+X-Y-Z	30g	-30g	-30g
QSL_-X+Y+Z	-30g	30g	30g
QSL_-X+Y-Z	-30g	30g	-30g
QSL_-X-Y+Z	-30g	-30g	30g
QSL_-X-Y-Z	-30g	-30g	-30g

Table 4. Random vibration loads

Bracket configuration	Frequency [Hz]	ASD [g^2/Hz]	Slope [dB/octave]	Acceleration G_{RMS}
Thrusters mounted	20	0.02	-	-
	100	0.2	4.31	2.84
	400	0.2	0	8.25
	2000	0.032	-3.43	13.54

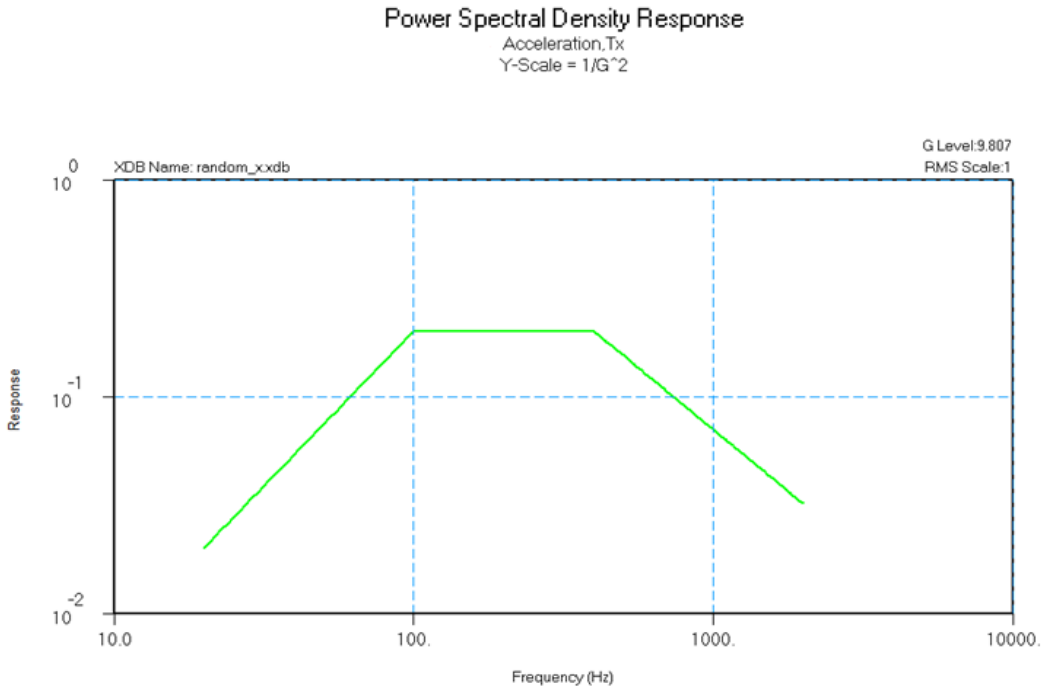

Fig. 2 ASD diagram

3. FEM MODEL DESCRIPTION

Regarding the stress analysis, a detailed FEM model was created. Element average size is 3 mm. For the idealization of the structure, the following elements were used in commercial software PATRAN-NASTRAN [8]:

- quadrilateral liniar element with shell property;
- bar elements for fasteners;
- punctiform concentrated mass elements for the thrusters;

The bolts were attached to the structure parts using RBE2 (Infinitly Rigid Bar Element with 2 nodes) elements.

The model was checked for duplicate elements, nodes, free boundaries, shell normals, material orienation, rigid body motion and is presented in Fig. 3. At the bracket-spacecraft interface, the model was clamped at the bottom edges as presented in Fig. 3, with SPC (Single Point Constraint equation for boundary conditions) in translations (translations were blocked) as can be seen from the figure. For better prediction of the joint stiffness, it was necessary to model the aluminium and composite parts with shell elements as well as the fasteners with beam elements.

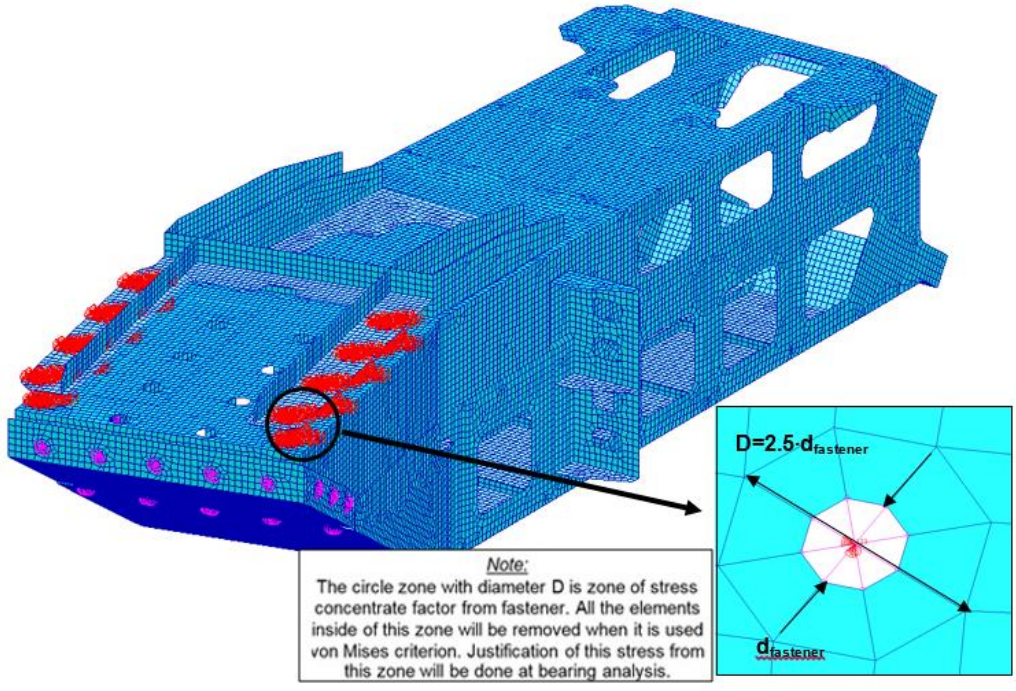

Fig. 3 Finite element model (FEM) with boundary conditions

The numerical analysis is used to obtain a global stresses field around each bolt and to identify the critical (most loaded) bolt under static or dynamic loading. The stress fields from FEM static and dynamic analysis are presented in Figs. 4 and 5.

The FEM results that are used in the procedure are the forces acting on each bolt under specified loading conditions.

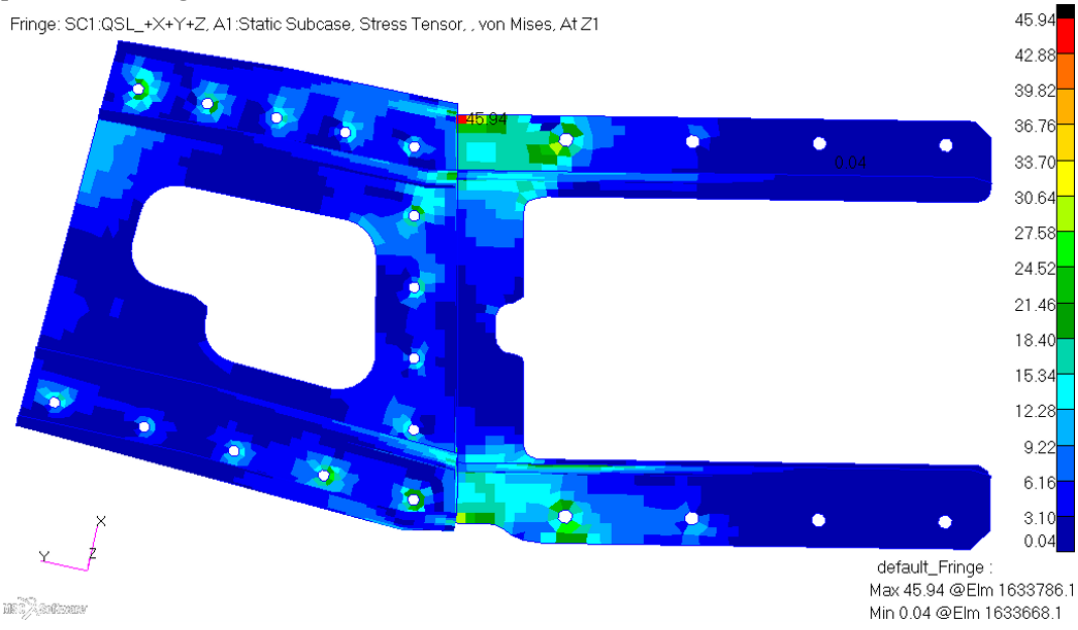

Fig. 4 Von Mises Stress Plot for the attachment, static analysis (max. 45.94 MPa)

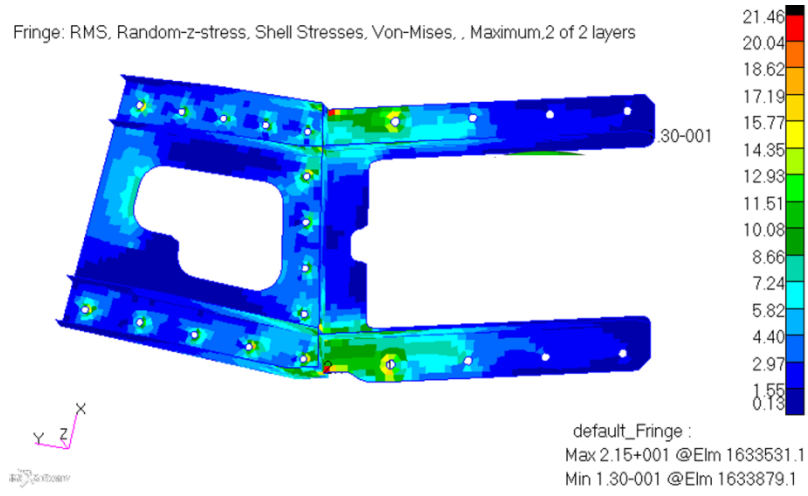

Fig. 5 Von Mises Stress Plot for the attachment, dynamic analysis (max. 21.46 MPa)

4. DESIGN METHODS

In this chapter, the design methods for the attachment hybrid joint of the bracket on the satellite composite platform are outlined in detailed. The type of bolts is standard threaded bolts with hexagonal head and nominal diameter of 4 mm. These bolts are made of A 286 standard steel DIN 65339-04006 [9] with LN 9161-04 [10] steel nuts and LN 9016-04L [10] steel washers. For better understanding, the joint configuration and bolt numbering is presented in Fig. 6. The most important geometrical parameters of the bolt are presented in Table 5, [11]. In the design process of a suitable joint strength establishment, the margin of safety can be written as follows [11]:

$$MoS = \frac{Allowable\ Load}{Limit\ Load \times FOS} - 1 \tag{1}$$

Limit Load is the maximum load in service and FOS is the factor of safety.

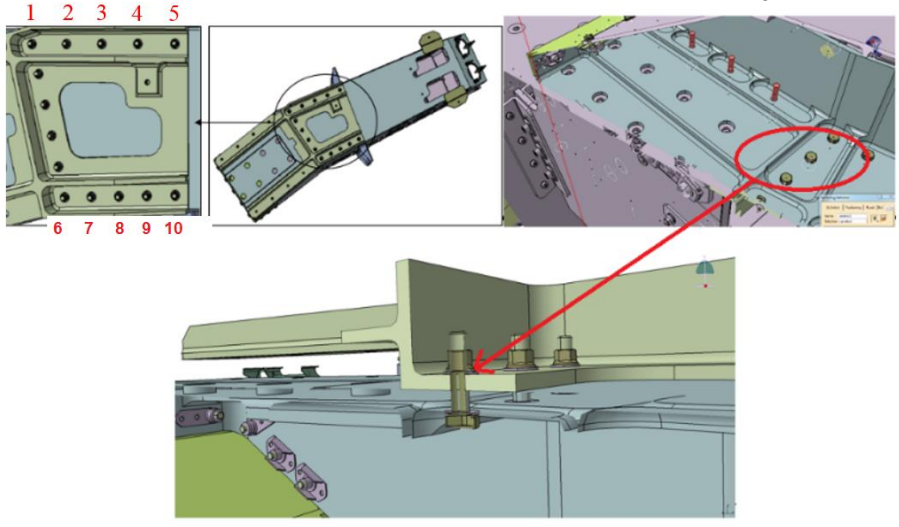

Fig. 6 Hybrid bolted joint, detailed view and bolt numbering

Table 5. Geometrical properties of M 4 thread bolts

Symbol	Unit	Description	Equation	Value
p	mm	pitch of the thread	-	0.7
H	mm	height of fundamental triangle	$0.866025 \cdot p$	0.606
d	mm	nominal fastener diameter	-	4
d_0	mm	diameter of the smallest cross-section of fastener shank	-	3.318
d_2	mm	pitch diameter	$d\text{-}2 \cdot 0.375 \cdot H$	3.545
d_3	mm	minor diameter of the fastener thread	$d\text{-}2 \cdot 0.5625 \cdot H$	3.318
d_S	mm	diameter used for stress calculation for MJ thread	$d_3\sqrt{2\text{-}\left(\frac{d_3}{d_2}\right)^2}$	3.518
d_{head}	mm	diameter of fastener head	-	8
D_h	mm	hole diameter of clamped parts	-	4.2
d_{uh}	mm	outside diameter at which under-head or under-nut frictional forces act	$0.5 \cdot (d_{head}+D_h)$	6.1
A_{nom}	mm^2	nominal cross-section area	$0.25 \cdot \pi \cdot d^2$	12.57
A_0	mm^2	minimum cross-section area	$0.25 \cdot \pi \cdot {d_0}^2$	8.65
A_3	mm^2	cross-sectional area at minor diameter of fastener thread	$0.25 \cdot \pi \cdot {d_3}^2$	8.65
A_s	mm^2	stress area calculation	$0.25 \cdot \pi \cdot {d_s}^2$	9.72
A_{uh}	mm^2	area under head/nut or washer that can be crushed	-	36.411

The following MoS's are applicable for static and dynamic analysis and are included in the design methodology for hybrid bolted joint failures [11].

- Joint separation (gapping) failure

The failure mode is defined to occur when the clamping force is reduced to its critical level, $F_{k,\,req}$ (which is greater than or equal to zero) and a small clearance appears between the attached plates. The MoS can be calculated as:

$$\mathrm{MoS_{sep}} = \frac{\mathrm{F_{V,min} - F_{K,req}}}{\left(1 - \mathrm{n}\left(\frac{\delta_c}{\delta_c + \delta_b}\right)\right) \cdot \mathrm{F_A} \cdot \mathrm{sf_{sep}}} - 1 \tag{2}$$

- Fastener failure due to preload and external loads

This failure criterion takes into account the maximum preload force and the axial force applied to the bolt shank:

$$\mathrm{MoS_{tot,b,y}} = \frac{\mathrm{A_S} \cdot \sigma_y}{\mathrm{F_{V,max}} + \Delta \mathrm{F_{b,A}} \cdot \mathrm{FOSY}} - 1, \text{ limit load} \tag{3}$$

$$\mathrm{MoS_{tot,b,u}} = \frac{\mathrm{A_S} \cdot \sigma_u}{\mathrm{F_{V,max}} + \Delta \mathrm{F_{b,A}} \cdot \mathrm{FOSU}} - 1, \text{ ultimate load} \tag{4}$$

- Thread failure by shear pull-out
  It refers to the pull-out failure of the thread by crushing:

$$\mathrm{MoS_{th,tot}} = \frac{\tau_u \cdot \pi \cdot D_1 \cdot \left(\frac{L_n - 0.8 \cdot p}{p}\right) \cdot \left[\frac{p}{2} + (d_2 - D_1) \cdot \tan(\theta)\right]}{F_{V,max} + \Delta F_{b,A} \cdot FOSU} - 1 \tag{5}$$

- Slipping of joint plates
  This failure mode refers to the relative movement of the plates when the friction load between the plates is overcome by the shear force applied to the joint:

$$\mathrm{MoS_{slip}} = \frac{\left(F_{V,min} - \left(1 - n\left(\frac{\delta_c}{\delta_c + \delta_b}\right)\right) \cdot F_A\right) \cdot \mu_s \cdot k}{F_Q \cdot FOSU} - 1 \tag{6}$$

- Fastener failure due to combined shear and axial loads
  The failure mode prediction takes into account the cumulative effect of combining shear and axial forces on the bolt shank:

$$R_{comb,y} = \sqrt{{R_{A,y}}^2 + {R_{Q,y}}^2} \leq 1 \tag{7}$$

$$R_{comb,u} = \sqrt{{R_{A,u}}^2 + {R_{Q,u}}^2} \leq 1 \tag{8}$$

$$R_{A,y} = \frac{F_{V,max} + \Delta F_{b,A} \cdot FOSY}{\sigma_y \cdot A_S} \tag{9}$$

$$R_{A,u} = \frac{F_{V,max} + \Delta F_{b,A} \cdot FOSU}{\sigma_u \cdot A_S} \tag{10}$$

$$R_{Q,y} = \frac{F_Q \cdot FOSY}{\tau_y \cdot A_S} \tag{11}$$

$$R_{Q,u} = \frac{F_Q \cdot FOSU}{\tau_u \cdot A_S} \tag{12}$$

$$\mathrm{MoS_{comb,y}} = \frac{1}{R_{comb,y}} - 1, \text{ limit load} \tag{13}$$

$$\mathrm{MoS_{comb,u}} = \frac{1}{R_{comb,u}} - 1, \text{ ultimate load} \tag{14}$$

where:

$F_{V,min}$ =1150 N- minimum preload force of the bolt [11],
$F_{V,max}$ =6400 N- maximum preload force of the bolt [11],
$F_{k,req}$ =0 N- minimum clamped force of the plates, [11],
n=0.5, non-dimensional factor taking into account the application point of the F_A,
δ_c, δ_b, - the clamped parts and bolt compliance:

$$\delta_b = \frac{1}{E_b}\left(\frac{L_{h,sub}}{A_{nom}} + \frac{L_{eng,sub}}{A_3} + \sum_{i=1}^{i=3} \frac{L_{sha,i}}{A_{sha,i}}\right) + \frac{L_{n,sub}}{E_n A_{nom}} \tag{15}$$

$$\delta_c = \frac{\frac{2}{w \cdot D_h \cdot \tan\phi} \ln\left[\frac{(D_{uh,brg} + D_h)(D_{avail} - D_h)}{(D_{uh,brg} - D_h)(D_{avail} + D_h)}\right] + \frac{4}{{D_{avail}}^2 - {D_h}^2}\left[L_c - \frac{D_{avail} - D_{uh,brg}}{w \cdot \tan\phi}\right]}{E_c \cdot \pi} \tag{16}$$

$L_{sha,i}$ – length of segment *i* of the bolt shank, see Fig. 7,
$A_{sha,i}$ – cross-section area of the segment *i* of the bolt shank, see Fig. 7,

$E_b=E_n=201000$ MPa elastic modulus of bolt and nut material,

E_c =71000 MPa (aluminum alloy), E_c =12000 MPa (CFRP) - elastic moduli of clamped parts.

For definition of lengths and diameters from relations (15) and (16) see Fig.7.

$\Delta F_{b,A}$ is axial bolt load due to external loads, it is an output from FEM analysis, see Fig.8.

$F_A=\frac{\Delta F_{b,A}}{n\left(\frac{\delta_c}{\delta_c+\delta_b}\right)}$, is external axial force acting on joint.

F_Q -shear bolt load, it is output by the FEM analysis, see Fig.8.

σ_y = 950 MPa, σ_u = 1100 MPa, τ_y = 570 MPa, τ_u = 655 MPa - yield and ultimate tensile and shear strength of the bolt [9].

sf_{sep} =1.4 - safety factor for separation, [11].

μ_s =0.37 - plates friction coefficient, experimentally determined.

k = 2- double lap joints,

FOSY = 1.25, FOSU=2, [12], factors of safety for limit and ultimate load cases.

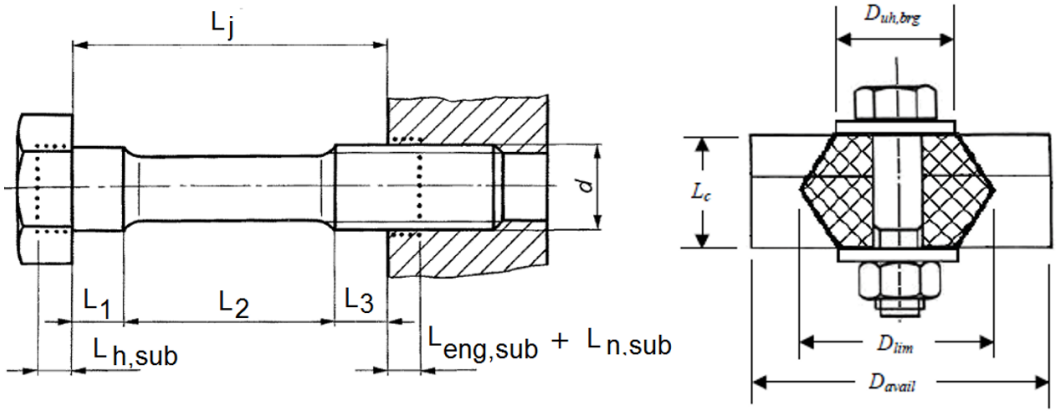

Fig. 7 Dimensions for bolt and clamped parts compliances

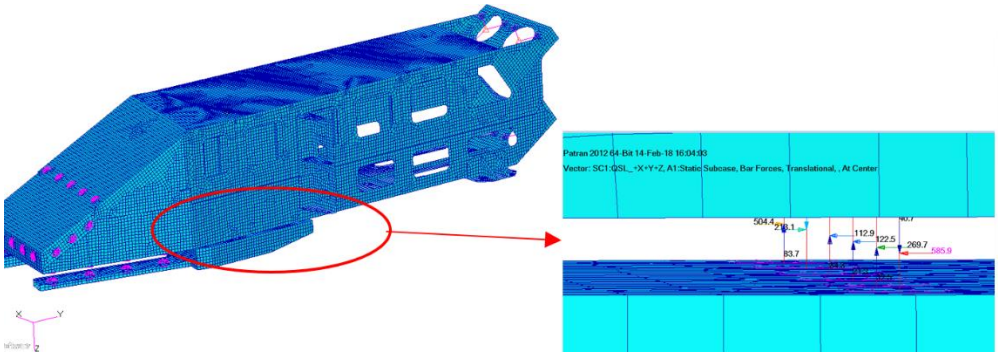

Fig. 8 Bolt forces $\Delta F_{b,A}$ and F_Q from FEM analysis

5. RANDOM VIBRATIONS

Random vibration analysis describes the forcing functions and the corresponding structural response statistically [13], [14]. It is generally assumed that the phasing of vibration at different frequencies is statistically uncorrelated. The amplitude of motion at each frequency is described by an Acceleration Spectral Density (ASD) function. In contrast to transient

analysis which predicts time histories of response quantities, random vibration analysis generates the Acceleration Spectral Density of these response quantities. From the Acceleration Spectral Density, the Root Mean Square (RMS) amplitude of the response quantity is calculated. The root-mean-square acceleration is the square root of the integral of the ASD acceleration over the frequency domain. Random vibration limit loads are typically taken as the "3-sigma load", obtained by multiplying the RMS load by load factor, j = 3.

In the dynamic analysis case, the Miles criterion (3σ) is used, that means in the formulas (1)-(14) external loads ($\Delta F_{b,A}$, F_Q) are multiplied by 3. It was used for analysis MSC Random software package compatible with MSC Nastran and MSC Patran [15]. The software uses the MSC Nastran ".xdb" output file from MSC Nastran frequency response analysis (SOL 111 solver) and then the analysis was executed from Patran using Tools/Random Analysis/Freq. Response. It has been performed 3 frequency response analysis, on one axis at a time (X, Y and Z axis) for each bracket, for further calculation of random response. Modal damping was taken 3% by engineering judgment. In Nastran, [15], the calculation of frequency response and its usage in random analysis are performed by separate modules. The equations of motion are assumed to be linear and the statistical properties of the random excitation are assumed to be stationary with respect to the time. It is calculated the Acceleration Spectral Density (ASD) of the response $S_j(\omega)$, which is the direct Fourier transform of auto-correlation or cross-correlation function $R_j(\tau)$ - see formulas (17) and (18):

$$R_j(\tau) = \lim_{T\to\infty} \frac{1}{T} \int_0^T u_j(t)\, u_j(t-\tau) dt \tag{17}$$

$$S_j(\omega) = \lim_{T\to\infty} \frac{2}{T} \left| \int_0^T e^{-i\omega t} u_j(t) dt \right|^2 \tag{18}$$

The following formula can be written:

$$U_j(\omega) = H_{ja}(\omega) \cdot Q_a(\omega) \tag{19}$$

This formula represents the structure response, $U_j(\omega)$ to an excitation $Q_a(\omega)$, if the answer function $H_{ja}(\omega)$ is known. From Parseval theorem the signal energy is defined as [13]:

$$E = \int_{-\infty}^{+\infty} |x(t)|^2 \, dt = \int_{-\infty}^{+\infty} |X(\omega)|^2 \, d\omega \tag{20}$$

In relation (20), $X(\omega)$ is the direct Fourier transform of the signal $x(t)$ and $|X(\omega)|^2$ represents the energy distribution of the signal as a function of frequency called energy spectral density. Taking into account the Parseval theorem and using the notations presented below for squaring left-right terms, from relation (19), $U_j(\omega)$ and $Q_a(\omega)$, [16]:

$$S_j(\omega) = |U_j(\omega)|^2 \tag{21}$$

$$S_a(\omega) = |Q_q(\omega)|^2 \tag{22}$$

The following relation is obtained:

$$S_j(\omega) = \left|H_{ja}(\omega)\right|^2 * S_a(\omega) \tag{23}$$

Knowing $S_j(\omega)$, the RMS values of the response $\bar{u}_j$ can be calculated [16]:

$$\bar{u}_j = [\frac{1}{4\pi}\sum_{i+1}^{N-1}[S_j(\omega_{i+1}) + S_j(\omega_i)](\omega_{i+1} - \omega_i)]^{1/2} \tag{24}$$

The response quantities $S_j(\omega)$ may be displacements, velocities, accelerations, internal forces, or stresses.

6. RESULTS

Using the numerical simulation results presented in Figs. 4, 5 and 8 in static and dynamic analysis, critical load cases can first be localized and then the shear forces on the bolts can be extracted. (F_Q in Table 6 and 7). The results for static and dynamic analysis for the most loaded bolts in shear and tension are presented in Tables 6-7.

Table 6. Static analysis results

Bolt type	Bolt nb. See Fig. 6	Load case	F_Q FEM (N)	$MoS_{tot,y}$	$MoS_{tot,u}$	$MoS_{th,tot}$	MoS_{sep}	MoS_{slip}	$MoS_{comb,y}$	$MoS_{comb,u}$
M 4	1	QSL+X+Y+Z	164.5	0.43	0.65	0.67	5.11	0.25		
	2	QSL_+X+Y-Z	416.3	0.42	0.63	0.66	3.17	-0.54	0.41	0.58
	3	QSL_-X-Y+Z	317.4	0.44	0.65	0.68	7.11	0.61		
	4	QSL_-X-Y-Z	409.5	0.42	0.63	0.65	2.57	-0.56	0.40	0.57
	5	QSL_+X+Y+Z	542.8	0.40	0.61	0.62	2.50	-0.52	0.38	0.55
	6	QSL_+X-Y-Z	168.6	0.44	0.65	0.68	7.11	0.61		
	7	QSL_-X+Y+Z	216.3	0.42	0.63	0.66	3.17	-0.54	0.41	0.58
	8	QSL_-X+Y-Z	383.5	0.43	0.65	0.67	5.11	0.25		
	9	QSL_-X-Y+Z	136.5	0.44	0.66	0.68	8.86	0.61		
	10	QSL_-X-Y-Z	384.5	0.40	0.61	0.57	8.21	-0.32	0.43	0.63

Table 7. Random vibration analysis results

Bolt type	Bolt nb. See Fig.6	Load case	F_Q FEM (N)	$MoS_{tot,y}$	$MoS_{tot,u}$	$MoS_{th,tot}$	MoS_{sep}	MoS_{slip}	$MoS_{comb,y}$	$MoS_{comb,u}$
M 4	1	RMS X	430	0.44	0.67	0.30	18.81	0.65		
	2	RMS X	289	0.44	0.67	0.30	21.18	1.22		
	3	RMS Z	107	0.43	0.65	0.29	6.16	-0.59	0.41	0.57
	4	RMS X	467	0.44	0.67	0.30	15.83	0.12		
	5	RMS Y	454	0.44	0.67	0.30	21.39	0.67		
	6	RMS Y	137	0.43	0.64	0.28	3.78	-0.71	0.38	0.51
	7	RMS X	521	0.44	0.66	0.30	13.28	0.01		
	8	RMS Z	153	0.44	0.67	0.30	15.84	0.54		
	9	RMS X	115	0.42	0.63	0.27	2.39	-0.75	0.37	0.48
	10	RMS Y	430	0.45	0.30	2.14	0.44	0.67		

Note: RMS X- the random vibration is perform only in X direction

The first observation from Tables 6 and 7 is that the negative values of MoS_{slip} do not mean failure of the joint; this denotes a relative displacement between the flanges of that joint. As a comparison between the static and dynamic analysis results, it can be observed

that some bolts (bolt 2 as an example) which have $MoS_{slip} < 0$ (relative displacement occurs) in static loading, have a complete different behavior in dynamic analysis ($MoS_{slip} > 0$).

The rest of the values for the margin of safety are positives which means all the joints studied are safe from the strength point of view and it can be concluded that the analytical algorithm which was originally developed for metal joints can be easily translated to hybrid metal - composite joints. In the Tables 6 and 7, the unfilled cells mean that the bolts are not subjected to shear and axial combining loads, due to the fact that the relative sliding between the flanges of the joint does not exist ($MoS_{slip} > 0$).

7. CONCLUSIONS

This paper presents an analytical set of relations that can be easily translated from metal joints to hybrid metal - composite joints in static or dynamic analysis of a real space application using the 2D FEM approach. It has been proved that the need of knowledge of their behavior under the static and dynamic load led to the elaboration of more detailed calculation methodologies for these hybrid joints. The space structure proposed for the study was a space thruster bracket, made of aluminum alloy metal, loaded in quasi-static and dynamic (random vibrations) environments and attached to the CFRP composite satellite platform. The proposed algorithm needs a local FEM model to simulate the loading conditions of the structure and to extract the loads acting on the bolts. The quasi-static loads were accelerations applied on all the three axis of the global coordinate system in the same time and the random vibration loads were introduced trough the Acceleration Spectral Density (ASD) diagram. The main objective of this paper is to validate the capability of the algorithm for predicting the three dimensional behavior of the hybrid joints in static and dynamic loading conditions. The major advantage of these design techniques is that they have the ability to incorporate and describe in detail the effects of important joining phenomena such as clamping, friction, clearance and relative displacement between plates of the joint, which are complex three-dimensional phenomena of major importance in the optimal design of hybrid bolted joints. Regarding the bolt clamping, it takes into account both the axial tension stress in the bolt shank and the stress due to the applied torque. In terms of friction, the design techniques can predict the relative sliding phenomenon of the plates, the slip that occurs when the shear force applied to the joint overcomes the frictional force between the plates and is described by the margin of safety MoS_{slip}. If this margin of safety is positive, the relative sliding is prevented, otherwise slipping between the plates will occur. The crushing of the surface of the plates under the bolt head is also predicted by these local computation techniques.

In terms of dynamic analysis, using RMS values from numerical simulation and Miles criterion (3σ), it was possible to study the behavior of the joints in random vibration environment. The author noticed the different behavior of joints in the case of static loading, as in some cases of M4 bolts (bolt number 2, as an example); thus the phenomenon of relative plate movement did not occur in static loading, whereas in the case of random vibrations this phenomenon was present.

The major contribution of the author in this paper is developing an easy to use approach, consisting of an analytic set of equations and a simplified 2D FEM model, for studying the structural response of the hybrid metal - composite joints to static and dynamic loading.

Thus, the design methods for hybrid metal-composite joints successfully described the local three-dimensional phenomena outlined above, making them a set of techniques that are important in the process of designing and optimizing the joints in a satellite space structure.

REFERENCES

[1] Ke. Liang, A global-local finite element analysis of hybrid composite-to-metal bolted connections used in aerospace engineering, *J. Cent. South Univ.*, vol. **24**, pp. 1225−1232, 2017.
[2] J. Lecomte, C. Bois, H. Wargnier, J.-C. Wahl, An analytical model for the prediction of load distribution in multi-bolt composite joints including hole-location errors, *Composite Structures*, no. 117, pp. 354–361, 2014.
[3] P. J. Gray, C. T. McCarthy, A global bolted joint model for finite element analysis of load distributions in multi-bolt composite joints, *Composites Part B*, vol. **41**, pp.317–325, 2010.
[4] F. Sen, K. Aldaş, Effects of using different metal materials on stresses in metal-composite hybrid joints, *Cantakaya Univ. Journ. Of Science and Engineering*, vol. **8**, pp. 1-13, 2011.
[5] F. Adel, S. Shokrollahi, M. Jamal-Omidi, H. Ahmadian, A model updating method for hybrid composite/aluminum bolted joints using modal test data, *Journal of Sound and Vibration*, vol. **396**, pp. 172-185, 2017.
[6] B. Andrade, J. P. B. Souza, J. M. L. Reis, H. S. da Costa Mattos, A temperature-dependent global failure criterion for a composite/metal joint, *Composites Part B*, vol. **137**, pp. 278-286, 2018.
[7] * * * MMPDS-05, Metallic Materials Properties Development and Standardization, 2010.
[8] * * * MSC Software, MSC Nastran Dynamic Analysis User's Guide, 2012.
[9] * * * DIN 65339 standard, Aerospace – Hexagon bolts, close tolerance, with short-length thread, 1998.
[10] * * *LN 9161 standard, Nuts hexagon flanged self-locking, 1977.
[11]* * *ECSS –E-HB-32-23A, Space engineering, Threaded fasteners handbook, ESA-ESTEC, 2010.
[12] * * *ECSS-E-30-Part 2A, Space Engineering, Mechanical, Part 2: Structural, ESA-ESTEC 2000.
[13] I. Magheti, *Mechanical Vibrations, Theory and Applications*, BREN, 2004.
[14] O. Rusu, *Metals Fatique*, vol 1 and 2, Technical, 1992.
[15] A. J. Davenport, M. Barbela, J. Leedom. *An Integrated Approach to Random Analysis Using MSC/PATRAN with MSC/NASTRAN*, 1999.
[16] I. Dima, C. Gh. Moisei, C. Coman, M. Nastase, C. Liliceanu, A. Petre, Comparative study between vibration and linear static analysis using Miles method for thruster brackets in space structures, *INCAS BULLETIN*, vol. **9**, issue 2, (online) ISSN 2247–4528, (print) ISSN 2066–8201, ISSN–L 2066–8201, DOI: 10.13111/2066-8201.2017.9.2.5, 2017.